Cytochrome aa_3 Electron-Transfer Reactions. Kinetics of Hexaammineruthenium(II) Reduction of the Beef Heart Enzyme

Robert A. Scott and Harry B. Gray*

Contribution No. 6083 from the Arthur Amos Noyes Laboratory of Chemical Physics, California Institute of Technology, Pasadena, California 91125. *Received July 26, 1979*

Abstract: The kinetics of anaerobic reduction of beef heart mitochondrial cytochrome *c* oxidase (cytochrome aa_3) by hexaammineruthenium(II) ($Ru(NH_3)_6^{2+}$) have been measured. The kinetics are biphasic at wavelengths in the Soret and at 605 nm, and neither phase exhibits (pseudo-)first-order behavior. A complete nonlinear optimization analysis shows that the slow phase obeys kinetics strictly second order in enzyme and zero order in $Ru(NH_3)_6^{2+}$; the fast phase, however, is apparently more complex. Kinetic difference spectra for the $Ru(NH_3)_6^{2+}$ reduction of native and cyanide-treated enzyme clearly demonstrate that the fast phase is due to reduction of heme a^{3+}, whereas the slow phase is due to reduction of heme a_3^{3+}. Analysis of the fast phase gives temperature-independent rate constants that are linearly dependent on $Ru(NH_3)_6^{2+}$ concentration. The slow phase is independent of $Ru(NH_3)_6^{2+}$ concentration with a second-order rate constant of $(1.04 \pm 0.06) \times 10^5$ $M^{-1}\cdot s^{-1}$ (25 °C) and activation parameters $\Delta H^{\ddagger} = 16.6 \pm 0.6$ kcal·mol^{-1}, $\Delta S^{\ddagger} = +20.2 \pm 2.0$ cal·deg^{-1}·mol^{-1} (pH 6.0 (cacodylate), $\mu = 0.10$ M) for native aa_3. The oxidized cyanide derivative yields a second-order rate constant of $(1.99 \pm 0.06) \times 10^4$ $M^{-1}\cdot s^{-1}$ (pH 6.0 (cacodylate), $\mu = 0.10$ M, 25 °C). The second-order dependence of the slow phase on enzyme concentration is interpreted as involving intermolecular electron transfer between $a^{2+}a_3^{3+}$ species, thereby resulting in reduction of heme a_3^{3+}.

Introduction

The terminal reaction of the mitochondrial electron transport chain is accomplished by cytochrome aa_3 (cytochrome *c* oxidase or ferrocytochrome *c*:O_2 oxidoreductase, EC 1.9.3.1). In this reaction, the enzyme accepts four reducing equivalents from its physiological reductant, cytochrome *c*, and transfers them to O_2, forming H_2O. The free energy released in this redox reaction is stored by conversion of 2 equiv of adenosine diphosphate (ADP) to adenosine triphosphate (ATP). The extreme importance of these reactions in physiological respiration has resulted in large expenditures of time and effort by many groups with the aim of answering structural and mechanistic questions concerning cytochome aa_3.

One of the more interesting questions to be answered is how the electrons are transferred within the enzyme during the catalytic cycle. The physiological reaction of cytochrome aa_3 with ferrocytochrome *c* is known to involve strong electrostatic interactions.[1-4] Since cytochrome *c* is a basic protein (i.e., positively charged at neutral pH), and is known to transfer electrons directly to heme a^{3+},[5-9] it is generally believed that the heme *a* region of the oxidase enzyme contains several anionic groups. The positively charged hexaaquochromium(II) ion also appears to reduce heme a^{3+} specifically.[10] In this case, reduction of the a_3^{3+} site was suggested to occur by intramolecular electron transfer from heme a^{2+}. A simple means of testing this interpretation involves the use of a different heme a^{3+} specific reagent, since the "intramolecular" electron-transfer rate constant observed should not depend on the reagent used. Owing to its positive charge, the outer sphere electron-transfer agent $Ru(NH_3)_6^{2+}$ was chosen for this study. Our analysis of the redox kinetics has revealed several new aspects of the electron-transfer behavior of cytochrome aa_3, not the least of which is the finding that the a^{2+} to a_3^{3+} transfer may occur by an *intermolecular* pathway.

Experimental Section

Materials and Equipment. Cacodylic acid (dimethylarsinic acid) was purchased from Matheson Coleman and Bell and was recrystallized before use by the published method.[11] 3-(*N*-Morpholino)propanesulfonic acid (Mops) was purchased from Sigma and used without further purification. Cholic acid was purchased from Sigma and purification prior to use was *required*. Briefly, the procedure involved decolorizing with activated charcoal and recrystallization from 95% ethanol. After purification, the cholic acid was dried to constant weight in vacuo and dissolved in water with a stoichiometric amount of KOH to give potassium cholate of the desired concentration. It was sometimes necessary to centrifuge this final solution to remove fine charcoal particles left from the purification steps.

The hexaammineruthenium(III) trichloride ($Ru(NH_3)_6Cl_3$) was from Matthey-Bishop (purchased through Alfa) and was recrystallized before use by a standard method.[12] Methyl viologen (MV, 1,1′-dimethyl-4,4′-bipyridinium dichloride) was purchased from Aldrich as the hydrate and used without further purification. The cation radical of methyl viologen ($MV^{+\cdot}$) was generated electrochemically by constant potential electrolysis of a 1 mM solution at ~−700 mV SCE and was used as an O_2 scavenger in a preflush of the Durrum D-110 stopped-flow apparatus to assure anaerobicity. Proflavin monohydrochloride was purchased from Polysciences, Inc., and was used without further purification. Proflavin was used as the photoacceptor of a $MV^{+\cdot}$-generating system which was used to scrub O_2 from Ar gas. The method used is a modification of the method suggested by Sweetser[13] and utilizes ethylenediaminetetraacetic acid (EDTA) as the electron donor. The scrubbing solution contained 50 μM proflavin, 0.5 mM MV, and 50 mM EDTA, and was made up in sodium phosphate buffer ($\mu = 0.1$, pH 7.0). Unless under an anaerobic atmosphere, this solution was stored in the dark to prevent ambient turnover of EDTA.

The nonionic detergent, Tween 20 (polyoxyethylene sorbitan monolaurate), was used as the solubilizing agent for cytochrome aa_3 for all the studies reported herein. Tween 20 was purchased from Sigma and was cleaned by passage through neutral alumina before use. The Tween 20 was stored as a 20% (w/v) solution at ~4 °C until needed. Just before use, the 20% Tween 20 was passed through a Millipore filter. The nonionic surfactant, Triton X-100, was purchased from Rohm and Haas Co. and was allowed to settle before using the top (less viscous) portion.

Horse heart cytochrome *c* was Sigma Type VI and was used without further purification. For the cytochrome *c* oxidase activity assays, cytochrome *c* was reduced with a tenfold excess of $Fe(EDTA)^{2-}$, and then dialyzed anaerobically to remove the excess reductant. Glucose oxidase was purchased from Sigma and was used without further treatment.

All other chemicals were obtained commercially and used without further purification. Distilled water was passed through a Barnstead Nanopure water purification system before use. The conductivity was routinely as high as 18 MΩ·cm.

Kinetics data were collected on a Durrum D-110 stopped-flow spectrophotometer modified for anaerobic work. The data were simultaneously displayed on a Tektronix 564B storage oscilloscope and temporarily stored in an analog input buffer (with built-in ADC).

0002-7863/80/1502-3219$01.00/0

Each set of data was subsequently sent under software control to a PDP-10 time-sharing computer system and written on disk for later analysis. The stop syringe and pneumatic ram of the D-110 were set such that the data acquisition was triggered approximately 10 ms before the actual stoppage of flow, so that an accurate measure (within ~2 ms) could be made of zero time.

Several parts of the Durrum flow system were modified so that the instrument could be used for anaerobic kinetics studies. The modifications included new syringe plungers and valve stems, hollowed to allow N_2 flushing behind the syringe plunger tips and valve tips during operation. The details of the modifications can be found elsewhere.[14]

Methods. Cytochrome *aa*$_3$. The enzyme was isolated from beef heart mitochondrial paste (A3 from the laboratory of D. E. Green) by the method of Hartzell and Beinert.[15] The final ammonium sulfate step results in a tight pellet of extremely concentrated (>1 mM) cytochrome aa_3 which is soluble in H_2O (without detergents) at high concentrations. The protein was thus stored as a highly concentrated solution in purified H_2O, frozen in liquid nitrogen. It is stable in this condition for an indefinite period. To avoid repetitive thawing of the enzyme, the concentrated solution was aliquotted by freezing individual drops in liquid nitrogen and storing it as such. The uniformity of the drops was sufficient to allow a certain number of drops to be thawed for each kinetics run, resulting in a fairly predictable enzyme concentration. Since the enzyme as stored is still associated with cholate, it was necessary to perform a detergent-exchange (to Tween 20) before use. The concentrated enzyme was treated with a few drops of concentrated (20% w/v) Tween 20 and loaded onto a small (~0.5 × 20 cm) G-25 column which was equilibrated with the buffer to be used for kinetics (with 0.1% Tween 20). The enzyme was then slowly eluted as a fairly tight band with the same buffer and was then diluted to the desired concentration. Since all the work described herein was performed at pH 6.0, it was found to be extremely important to obtain complete exchange of Tween 20 for cholate, since any residual cholate has a tendency to make the solution turbid. (Cholate has a pK of ~6.4[16] and the acid form is relatively insoluble in water.)

Protein concentrations were determined by the Lowry method[17] and enzyme preparations routinely exhibited heme/protein ratios of ~12 nmol of heme/mg of protein. The cytochome *c* oxidase activity of the enzyme was measured spectrophotometrically using a slight modification of a standard method.[18] The assay was performed in Mops buffer at pH 7.0, μ = 0.1 M. The ferrocytochrome *c* was generated by $Fe(EDTA)^{2-}$ as described above and was diluted to an initial concentration of ~15 μM. The assay was performed at 25 °C in a total volume of 2 mL. The molecular activity (MA) in units of μM ferrocytochrome *c* oxidized·(μM cytochome aa_3)$^{-1}$·s^{-1} is given by (e.g., see ref 19 and 20):

$$\mathrm{MA} \equiv k_{\mathrm{obsd}}[\mathrm{cyt}\ c^{2+}]_0/[\mathrm{cyt}\ aa_3]$$

where k_{obsd} is the first-order rate constant measured for the decay of A_{550}, $[\mathrm{cyt}\ c^{2+}]_0$ is the initial concentration of ferrocytochrome *c*, and $[\mathrm{cyt}\ aa_3]$ is the concentration of the enzyme. Values of the molecular activity for the Hartzell and Beinert preparations used for the present studies were usually ~100 s^{-1} and were unchanged after more than a day at room temperature.

Although the anaerobic modifications to the Durrum helped significantly in reducing the level of O_2 in the system, it was not possible to consistently achieve an O_2 concentration low enough for examination of "anaerobic" kinetics with cytochrome aa_3. Thus, short periods of steady-state behavior were observed in some cases when the anaerobicity was not optimal. For this reason, the final traces of O_2 were scavenged from the reactant solutions with the glucose/glucose oxidase system.[21,22] Glucose was added to all buffers to a final concentration of 50 mM and glucose oxidase was added to a final concentration of ~0.1–0.2 unit/mL *after* the solutions were degassed. Since the amount of O_2 scavenged by the glucose oxidase under these conditions should be minimal, it was considered unnecessary to add catalase to clean up the small amount of H_2O_2 formed.

The protein solution was degassed by several pump/flush cycles (with Ar) with continuous stirring while on ice. The evacuation was carefully controlled to avoid excessive foaming of the protein–detergent solution during degassing. After the first pumping cycle, glucose oxidase was added to the enzyme solution and the degassing procedure was then completed.

The cyanide derivative of oxidized cytochrome aa_3 was prepared by incubating the enzyme in (a final concentration of) 15 mM (500-fold excess) NaCN. Since cyanide reacts only very slowly with oxidized cytochome aa_3,[19,23,24] the sample was allowed to incubate overnight at room temperature at a high concentration of enzyme. The complete formation of the cyanide–enzyme complex was checked spectrophotometrically before performing kinetics with this derivative.

Hexaammineruthenium(II) Reagent. $Ru(NH_3)_6^{2+}$ stock solutions were prepared by electrochemical reduction of the Ru(III) complex at a Pt electrode. Constant potential coulometry was performed at a potential of −300 mV SCE (~100 mV below the $E^{\circ\prime}$ of the Ru(II,III) couple, 50 mV NHE). The stock solution usually consisted of 0.5 mM $Ru(NH_3)_6^{2+}$ in the appropriate buffer (see below) in the absence of Tween 20. (Tween 20 was added to the buffers used for dilution of the Ru(II) stock solution, since the presence of this detergent in the stock solution caused fouling of the electrode.) Electrolysis was carried out until the charge passed had stopped accumulating (~3–4 h under well-stirred conditions with a Pt gauze working electrode and a coiled Pt wire counter electrode), but the stock Ru(II) solution was maintained at −300 mV SCE throughout the kinetics run to minimize any reoxidation. Since $Ru(NH_3)_6^{2+}$ is susceptible to aquation, the $Ru(NH_3)_6Cl_3$ was dissolved in buffer immediately prior to electrochemistry, and the Ru(II) complex was used for kinetics as soon as possible after reduction. In no instance was the $Ru(NH_3)_6^{2+}$ solution older than ~10 h when used for kinetics. The Ru(II) complex also seems to be less stable (presumably toward aquation) at pH 7 than at pH 6 and since the pH optimum of cytochome *c* oxidase activity is also ≲6, all kinetics were performed at pH 6.

Once the $Ru(NH_3)_6^{2+}$ stock solution was prepared, various concentrations were obtained by diluting aliquots of the stock solution into the appropriate buffer (which had already been degassed by Ar bubbling). All transfers were performed in a Hamilton gas-tight syringe with a gas flush modification that was kept under Ar flow at all times.

Kinetics. The reduction of cytochrome aa_3 by $Ru(NH_3)_6^{2+}$ always exhibited biphasic kinetics with the fast phase taking place on the millisecond time scale. Owing to the large rate constant for this fast phase, the range of $Ru(NH_3)_6^{2+}$ concentration achievable was limited. Concentration dependences were performed over the range 0.04–0.20 mM. Fast phase rates at concentrations higher than 0.20 mM were too fast for accurate measurement and it was found to be very difficult to keep $Ru(NH_3)_6^{2+}$ solutions of concentrations less than 0.04 mM completely reduced. The enzyme concentration was usually ~2.8 μM (5.6 μM heme), but in some cases was varied from 1.4 to 3.0 μM. Thus, $Ru(NH_3)_6^{2+}$ was always present in pseudo-first-order excess over cytochome aa_3.

All kinetics were performed in cacodylate buffer at pH 6.0 with a total ionic strength of 0.1 M. The cacodylate buffer (adjusted with NaOH) contributed 0.05 M to the ionic strength with the rest being made up by $Ru(NH_3)_6^{2+}$ and an inert salt (Na_2SO_4). The Tween 20 concentration (for solubilization of the enzyme and added to reagent solutions to avoid Schlieren effects in the observation chamber) was varied from 0.05 to 0.50% (w/v) without observable effect on the kinetics. Depending on the extent of detergent exchange and on the final Tween 20 concentration, some turbidity was observed in the enzyme solution during kinetics runs. Except for a higher background absorbance (due to scattering), this turbidity did not seem to affect the kinetics observed, indicating that it probably did not involve enzyme denaturation. However, none of the kinetics results obtained with turbid enzyme solution was used in the final analysis.

Temperature equilibration was obtained by use of a circulating constant temperature bath (Forma), and the temperature was measured next to the syringe barrels in the Durrum bath to assure accuracy. In general, the temperatures quoted for the temperature dependence data are good to within ±0.1 °C (and ±0.05 °C at 25 °C). The enzyme reservoir flask was kept jacketed with a flexible plastic bag filled with ice throughout the experiment, and both enzyme and reagent solutions were allowed to equilibrate for 15–20 min in the syringes before each kinetics run.

The Ar gas used for degassing and purging was passed through a MnO/vermiculite tower and then through a train of proflavin/methyl viologen gas scrubbers before use. The MnO tower was ~24 in. long × ~3 in. in diameter and the MnO/vermiculite was prepared by a published procedure.[25] Reduced methyl viologen ($MV^{+\cdot}$) was generated by illumination of the proflavin–MV–EDTA gas scrubbers while bubbling with Ar. Once generated, room light was sufficient to maintain a level of $MV^{+\cdot}$ sufficient for scavenging any O_2 left over from the MnO tower.

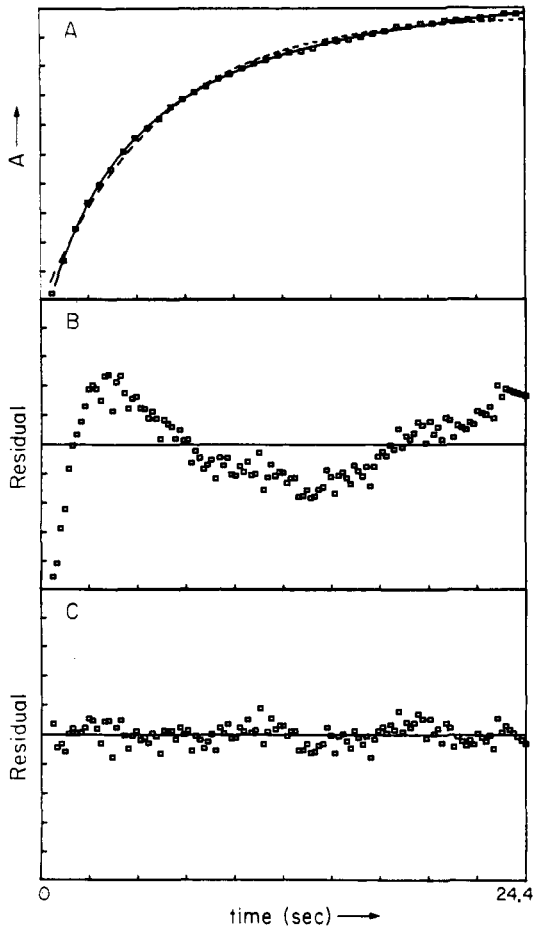

Figure 1. Typical absorbance–time fits to the slow phase. Only the slow phase was fit (to either a first- or second-order decay). (A) Original absorbance vs. time data (□, 120 points acquired, every third point plotted) with best first-order fit (- - -) and best second-order fit (—) (B) Residuals (data minus fit) for the first-order fit in A. (C) Residuals (data minus fit) for the second-order fit in A. (Plots B and C are on the same scale.)

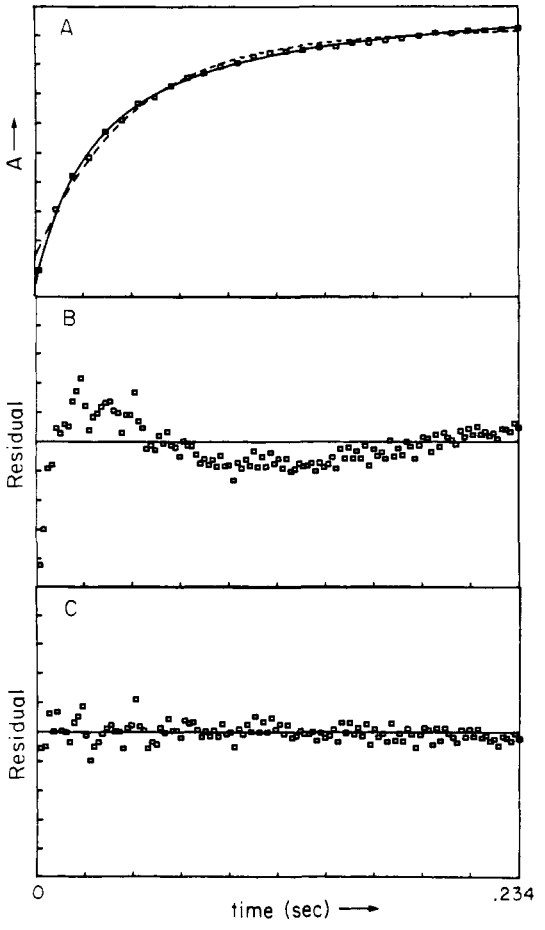

Figure 2. Typical absorbance–time fits to the fast phase. The total fit consisted of a slow-phase second-order decay plus a fast-phase first- or second-order decay. (A) Original absorbance vs. time data (□, 122 points acquired, every fourth point plotted) with best first-order fit (- - -) and best second-order fit (—) (B) Residuals (data minus fit) for the first-order fit in A. (C) Residuals (data minus fit) for the second-order fit in A. (Plots B and C are on the same scale.)

Kinetics Analysis. Owing to the complexity of the kinetics observed for the reduction of cytochrome aa_3 by $Ru(NH_3)_6^{2+}$, standard kinetics analytical techniques were inadequate. A computer program (KINPRO) was written to analyze complicated kinetics progress curves using an iterative nonlinear least-squares method based on the Newton–Gauss approach. This program will fit kinetics data to a sum of up to four separate kinetics functions, this sum being any combination of first-order, second-order approach to equilibrium, or two-reactant second-order decays. The program optimizes all parameters, including the infinity absorbance and preexponential constants, and proved ideal for this study since biphasic kinetics of non-first-order decays were always observed. The program is described in more detail elsewhere.[14] Plots of absorbance vs. time along with fits and residuals plots were all performed on a Tektronix 4010-1 Graphics terminal interfaced to a PDP-10 time-sharing computer system.

Results

The reduction of cytochrome aa_3 by electrochemically generated hexaammineruthenium(II) ($Ru(NH_3)_6^{2+}$) was observed to to be biphasic at 444 nm (reduced Soret maximum) and at 605 nm (reduced α maximum). At 444 nm, both phases contribute approximately equally to the total change in absorbance (ΔA), but preliminary results at 605 nm indicate that the fast phase contributes ~75–80% of the total ΔA. All of the rate constants reported herein were measured at 444 nm.

Initial attempts at fitting the slow phase (data collected over ~20 s) to a standard first-order exponential decay resulted in rather poor fits (large χ^2 values), and analyses by the Guggenheim method[26] always predicted infinity-absorbance values that were significantly different from those observed. For this reason, attempts were made to fit the slow phase data to other possible kinetics functions (e.g., second-order decay, approach to equilibrium). Figure 1 shows the fit of the slow phase data to both first-order and second-order decays. By examination of the residuals (data minus fit) for both functions, it can be concluded that a second-order decay is involved (rather than a first-order decay).

Although the slow phase was easily analyzed without interference from the fast phase (by simple deletion of a few initial data points), analysis of the fast phase required the ability to fit both phases simultaneously. With the aid of KINPRO (see Experimental Section), it was found that fits of data sets covering both phases (with equal numbers of points in each phase) to functions consisting of a fast first-order decay and slow second-order decay did not reproduce the data as well as a fit that assumes both fast and slow second-order decays (Figure 2).[27]

In order to characterize more fully the nature of the observed biphasicity, the wavelength dependence (in the Soret region) of the amplitudes of the respective phases was studied by measuring the kinetics at several discrete wavelengths between ~390 and ~460 nm. These kinetic difference spectra are displayed in Figure 3 for both the native enzyme and the oxidized-cyanide derivative (aa_3-CN). From Figure 3, it can be seen that the fast phase appears insensitive to the effect of cyanide, whereas the slow-phase difference spectrum is considerably different for the reaction with aa_3-CN.

The dependence of the observed fast (second order) and slow

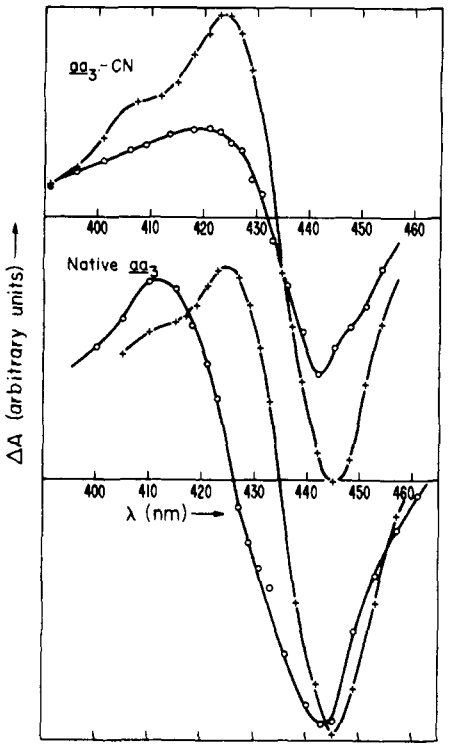

Figure 3. Kinetic difference spectra (Soret) for both phases of the reactions between $Ru(NH_3)_6^{2+}$ and native cytochrome aa_3 (lower) and $Ru(NH_3)_6^{2+}$ and the cyanide derivative of oxidized cytochrome aa_3 (upper). The plotted points represent the preexponential constants calculated for a particular wavelength: (+) fast phase; (○) slow phase. The absolute ΔAs are arbitrary, but within each half of the figure, the ΔAs are relatively correct.

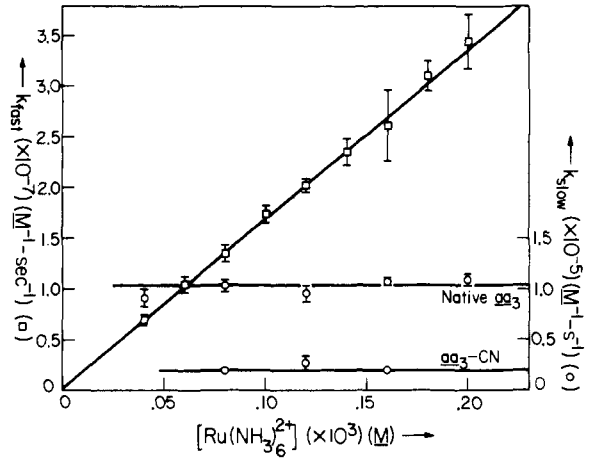

Figure 4. $[Ru(NH_3)_6^{2+}]$ dependence of k_{fast} and k_{slow} for the reduction of cytochrome aa_3 by $Ru(NH_3)_6^{2+}$. The lines are the best first- and zero-order least-squares fits to the fast (□) and slow (○) phases, respectively. See text for fit parameters.

rate constants on $[Ru(NH_3)_6^{2+}]$ is illustrated in Figure 4, and the data are collected in Table I. Each pair of (fast and slow) rate constants in Table I is the weighted mean of about three or more determinations. Each determination was the mean of at least four separate runs, and each run consisted of at least one slow-phase and two fast-phase scans, the fast-phase scans being signal averaged and spliced to the slow-phase scan before being analyzed by KINPRO. From Figure 4 it can be seen that the fast phase analyzed as a second-order decay is first order in $Ru(NH_3)_6^{2+}$. The slope of the best linear least-squares fit gives a third-order rate constant (for the fast phase) of $(1.68 \pm 0.02) \times 10^{11}$ M^{-2} s^{-1} (pH 6.0 (cacodylate), μ = 0.1 M, 25 °C). Analysis of the fast phase as a first-order decay yields a

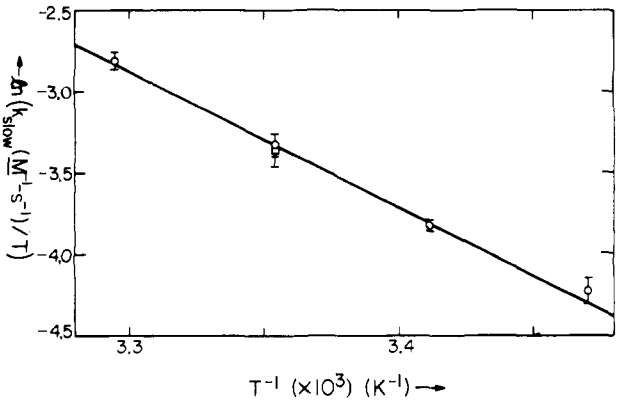

Figure 5. Eyring plot of the slow-phase rate constants for $Ru(NH_3)_6^{2+}$ reduction of native cytochrome aa_3: (○) $[Ru(NH_3)_6^{2+}]$ = 0.12 mM; (□) value calculated from $[Ru(NH_3)_6^{2+}]$ dependence.

Table I. Rate Constants for $Ru(NH_3)_6^{2+}$ Reduction of Cytochrome aa_3

aa_3 derivative	$[Ru(NH_3)_6^{2+}]$, mM	T, °C	$k_{fast} \pm \sigma$ (×10⁻⁶), $M^{-1}\cdot s^{-1}$	$k_{slow} \pm \sigma$ (×10⁻⁴), $M^{-1}\cdot s^{-1}$
native	0.04	25.0	7.01 ± 0.49	9.10 ± 0.82
native	0.06	25.0	10.5 ± 0.8	
native	0.08	25.0	13.5 ± 0.8	10.4 ± 0.5
native	0.10	25.0	17.4 ± 0.8	
native	0.12	25.0	20.2 ± 0.7	9.60 ± 0.75
native	0.14	25.0	23.6 ± 1.3	
native	0.16	25.0	26.2 ± 3.5	10.7 ± 0.4
native	0.18	25.0	31.1 ± 1.5	
native	0.20	25.0	34.6 ± 2.7	10.9 ± 0.6
native	0.12	12.0	15.7 ± 0.8	
native	0.12	15.0	17.7 ± 0.3	4.20 ± 0.34
native	0.12	20.0	19.0 ± 0.8	6.39 ± 0.19
native	0.12	25.0	16.5 ± 1.6	10.7 ± 0.4
native	0.12	30.4	18.9 ± 2.4	18.2 ± 1.0
aa_3-CN	0.08	25.0	12.0 ± 0.7	1.98 ± 0.08
aa_3-CN	0.12	25.0	14.2 ± 1.0	2.71 ± 0.73
aa_3-CN	0.16	25.0	25.3 ± 1.5	1.99 ± 0.11

$[Ru(NH_3)_6^{2+}]$ dependence characterized by a second-order rate constant of $\sim 5 \times 10^5$ M^{-1} s^{-1}. Although the fast-phase rate constants for $Ru(NH_3)_6^{2+}$ reduction of the oxidized cyanide derivative are less well determined, they are very similar to those for the reduction of native aa_3.

Figure 4 also shows the $[Ru(NH_3)_6^{2+}]$ dependence of the slow-phase rate constants. Over the $[Ru(NH_3)_6^{2+}]$ range available, the rate of the slow phase is independent of the reductant concentration with a second-order rate constant of $(1.04 \pm 0.06) \times 10^5$ M^{-1} s^{-1} for native aa_3 and $(1.99 \pm 0.06) \times 10^4$ M^{-1} s^{-1} for aa_3-CN (pH 6.0 (cacodylate), μ = 0.1 M, 25 °C). Thus, the binding of cyanide to aa_3 results in a decrease in the rate of the slow phase by a factor of $\sim$5 and also alters the corresponding kinetic difference spectrum (Figure 3).

The temperature dependences of the rate constants for both the fast and slow phases (for $Ru(NH_3)_6^{2+}$ reduction of native aa_3) are given in Table I, and the Eyring plot for the slow phase is shown in Figure 5. Examination of the rate constants in Table I reveals that the fast phase is temperature independent within experimental error ($\Delta H^{\ddagger}$ = 0.4 ± 1.2 kcal·mol^{-1}). The activation parameters for the slow phase of $Ru(NH_3)_6^{2+}$ reduction of native aa_3 (calculated from Figure 5) are $\Delta H^{\ddagger}$ = 16.6 ± 0.6 kcal·mol^{-1} and $\Delta S^{\ddagger}$ = 20.2 ± 2.0 eu (pH 6.0 (cacodylate), μ = 0.1 M, $[Ru(NH_3)_6^{2+}]$ = 0.12 mM). The averaged second-order rate constant for the slow phase taken

from the $[Ru(NH_3)_6^{2+}]$-dependence data is also indicated in Figure 5.

Discussion

The initial phase observed for the reduction of cytochrome aa_3 by $Ru(NH_3)_6^{2+}$ is fast (occurring over $\lesssim$100 ms even at submillimolar concentrations of reductant). We attribute this rapid rate to the positive charge of the reductant, since preliminary results indicate that reduction of aa_3 by $Ru(NH_3)_5py^{2+}$ (py = pyridine) is also fast ($t_{1/2} \simeq$ 140 ms at [Ru(II)] = 0.1 mM), whereas reduction by $Fe(EDTA)^{2-}$ (EDTA = ethylenediaminetetraacetate) ($t_{1/2} \simeq$ 500 s at [Fe(II)] = 0.1 mM), $Fe(dipic)_2^{2-}$ (dipic = 2,6-dipicolinate) ($t_{1/2} \simeq$ 10 s at [Fe(II)] = 0.1 mM), or $Fe(CDTA)^{2-}$ (CDTA = *trans*-1,2-cyclohexanediaminetetraacetate) ($t_{1/2} \simeq$ 15 s at [Fe(II)] = 0.1 mM) is much slower.[28]

Several independent lines of evidence support the assignment of the fast phase of the $Ru(NH_3)_6^{2+}$ reaction to the reduction of a^{3+} (and the slow phase to reduction of a_3^{3+}). First, the kinetic difference spectrum of the fast phase (see Figure 3) is essentially unaltered upon binding of cyanide to the enzyme (it is well established that cyanide binds to a_3^{3+}), whereas the addition of cyanide causes drastic changes in the slow-phase kinetic difference spectrum. In addition, the rate constants reflect the same type of response to the addition of cyanide, the slow-phase rate constants diminishing by a factor of ~5, whereas the fast-phase rate constants remain unchanged. Preliminary experiments at 605 nm also indicate that (for $Ru(NH_3)_6^{2+}$ reduction of the native enzyme) the fast phase contributes ~75–80% of the total ΔA. It is fairly well established[10,29,30] that cytochrome *a* contributes ~80–100% of the ΔA at 605 nm. Comparison of the kinetic difference spectra with published difference spectra that have been previously assigned separate cytochrome *a* and a_3 contributions[10,30] completely corroborates the assignment of the fast phase to heme a^{3+} reduction and the slow phase to the reduction of heme a_3^{3+}.

Although the results shown in Figure 2 indicate that the fast phase is apparently second order in enzyme concentration, a comparison of the residuals in Figures 1 and 2 suggests that this conclusion is not as strong as for the slow phase. The temperature independence of the fast-phase rate constants also argues against the involvement of any significant enzyme–enzyme interaction (vide infra). For these reasons, a discussion of the reasonable mechanistic alternatives for the fast phase will be deferred until further experimentation defines the exact nature of the kinetics decay.[31]

Let us now consider mechanistic interpretation of the slow phase. Since all the a^{3+} has been reduced in the fast phase, the initial conditions for the slow phase can be assumed to involve a pool of $a^{2+}a_3^{3+}$ enzyme. The simplest interpretation of the second-order behavior of the slow phase involves a mechanism wherein two molecules of $a^{2+}a_3^{3+}$ exchange electrons (i.e., heme a_3^{3+} of one molecule accepts electrons from heme a^{2+} of the other):[32]

$$a^{2+}a_3^{3+} + a^{2+}a_3^{3+} \xrightarrow{k_{slow}} a^{2+}a_3^{2+} + a^{3+}a_3^{3+}$$

Any oxidized enzyme formed by this process would be immediately consumed by the excess $Ru(NH_3)_6^{2+}$ in a process identical with that involved in the fast phase. Thus, the only detectable change would be the reduction of one a_3^{3+} (as is observed in the slow phase). Since the electron transfer in this mechanism is *intermolecular*, the rate law would be second order in enzyme (as observed). It should also be mentioned that the activation parameters for the slow phase support some type of strong enzyme–enzyme interaction (probably involving conformational changes and displacement of ordered solvent structure).[33,34]

We note in closing that analysis of the present slow-phase data as a first-order decay yields a rate constant of ~0.2–0.4 s^{-1} (which is independent of the $Ru(NH_3)_6^{2+}$ concentration). This rate constant is remarkably similar to that reported for the slow phase of the biphasic Cr^{2+} reduction of cytochrome aa_3.[10] We believe it is possible that a second-order process with a rate constant of about 10^5 $M^{-1}\cdot s^{-1}$ might also explain the slow-phase $[Cr^{2+}]$-independent kinetics. If the slow phases observed in the $Ru(NH_3)_6^{2+}$ and Cr^{2+} reductions are indeed second order in enzyme, then studies in which the initial enzyme concentration is varied over a suitably wide range should provide confirmatory evidence. Experiments along these lines are planned.

Acknowledgment. The authors thank Professor Helmut Beinert and Dr. Robert Shaw for help with the enzyme purification. Professor Martin Kamen made many helpful suggestions in the early stages of our work. R.A.S. acknowledges a National Science Foundation Graduate Fellowship (1975–1978) and a National Institutes of Health Traineeship (1978–1979). This research was supported by National Science Foundation Grant No. CHE77-11389.

References and Notes

(1) Davies, H. C.; Smith, L.; Wasserman, A. R. *Biochim. Biophys. Acta* **1964**, *85*, 238.
(2) Maurel, P.; Douzou, P.; Waldmann, J.; Yonetani, T. *Biochim. Biophys. Acta* **1978**, *525*, 314.
(3) Nicholls, P.; Chance, B. "Molecular Mechanisms of Oxygen Activation", Hayaishi, O., Ed.; Academic Press: New York, 1974; p 479.
(4) Takemori, S.; Wada, K.; Ando, K.; Hosokawa, M.; Sekuzu, I.; Okunuki, K. *J. Biochem. (Tokyo)* **1962**, *52*, 28.
(5) Andréasson, L.-E.; Malmström, B. G.; Strömberg, C.; Vanngård, T. *FEBS Lett.* **1972**, *28*, 297.
(6) Antonini, E.; Brunori, M.; Greenwood, C.; Wilson, M. T. *Biochem. Soc. Trans.* **1973**, *1*, 34.
(7) Andréasson, L.-E. *Eur. J. Biochem.* **1975**, *53*, 591.
(8) Gibson, Q. H.; Greenwood, C.; Wharton, D. C.; Palmer, G. *J. Biol. Chem.* **1965**, *240*, 888.
(9) Wilson, M. T.; Greenwood, C.; Brunori, M.; Antonini, E. *Biochem. J.* **1975**, *147*, 145.
(10) Greenwood, C.; Brittain, T.; Brunori, M.; Wilson, M. T. *Biochem. J.* **1977**, *165*, 413.
(11) Perrin, D. D.; Armarego, W. L. F.; Perrin, D. R. "Purification of Laboratory Chemicals"; Pergamon Press: New York 1966; p 294.
(12) Pladziewicz, J. R.; Meyer, T. J.; Broomhead, J. A.; Taube, H. *Inorg. Chem.* **1973**, *12*, 639.
(13) Sweetser, P. B. *Anal. Chem.* **1967**, *39*, 979.
(14) Scott, R. A. Ph.D. Thesis, California Institute of Technology, Pasadena, 1980.
(15) Hartzell, C.; Beinert, H. *Biochim. Biophys. Acta* **1974**, *368*, 318.
(16) van Gelder, B. F.; van Rijn, J. L. M. L.; Schilder, G. J. A.; Wilms, J. "Structure and Function of Energy-Transducing Membranes", van Dam, K. van Gelder, B. F., Eds.; Elsevier, North-Holland: Amsterdam, 1977; p 61.
(17) Lowry, O. H.; Rosebrough, N. J.; Farr, A. L.; Randall, R. J. *J. Biol. Chem.* **1951**, *193*, 265.
(18) Smith, L. "Methods of Biochemical Analysis", Glick, D., Ed.; Interscience: New York, 1955; Vol. II, p 427.
(19) van Buuren, K. J. H.; Zuurendonk, P. F.; van Gelder, B. F.; Muijsers, A. O. *Biochim. Biophys. Acta* **1972**, *256*, 243.
(20) Vanneste, W. H.; Ysebaert-Vanneste, M.; Mason, H. S. *J. Biol. Chem.* **1974**, *249*, 7390.
(21) Peterson, J. A.; White, R. E.; Yasukochi, Y.; Coomes, M. L.; O'Keeffe, D. H.; Ebel, R. E.; Masters, B. S.; Ballou, D. P.; Coon. M. J. *J. Biol. Chem.* **1977**, *252*, 4431.
(22) Ballou, D. P.; Veeger, C.; van der Hoeven, T. A.; Coon, M. J. *FEBS Lett.* **1974**, *38*, 337.
(23) van Buuren, K. J. H.; Nicholls, P.; van Gelder, B. F. *Biochim. Biophys. Acta* **1972**, *256*, 258.
(24) Antonini, E.; Brunori, M.; Greenwood, C.; Malmström, B. G.; Rotilio, G. C. *Eur. J. Biochem.* **1971**, *23*, 396.
(25) Shriver, D. F. "The Manipulation of Air-Sensitive Compounds"; McGraw-Hill: New York, 1969; p 199.
(26) Guggenheim, E. A. *Philos. Mag.* **1926**, *2*, 538.
(27) In our view, the reason that such complex kinetics have not been reported previously is related to the analytical techniques currently in common use by most kineticists. The standard first-order kinetics analysis has become so widely accepted that workers tend to apply it exclusively to cases in which a more thorough survey is desirable. Indeed, the two fits shown in Figure 1 are close enough that, without a check of the residuals (which is often not performed), the simpler first-order fit might be judged satisfactory. However, it is clear from the residuals plot of Figure 1 that the slow phase obeys second-order kinetics.
(28) The $t_{1/2}$ values reported were calculated *assuming* first-order kinetics were obeyed in each case. This assumption may or may not be valid for these reactions. The numbers are quoted only to indicate the relative rates of

the reactions (Scott, R. A., unpublished results).
(29) Yu, C.-A.; Yu, L. *Biochem. Biophys. Res. Commun.* **1976**, *70*, 1115.
(30) Gilmour, M. V.; Wilson, D. F.; Lemberg, R. *Biochim. Biophys. Acta* **1967**, *143*, 487.
(31) However, we emphasize at this time that one such reasonable alternative is a simple bimolecular mechanism involving electron transfer from $Ru(NH_3)_6^{2+}$ to a^{3+}.
(32) The intermolecular redox process could also involve a reduced copper site as the primary electron donor to a_3^{3+} ($a^{2+}a_3^{3+}$(red Cu) + $a^{2+}a_3^{3+} \rightarrow$ (k_{slow}) $a^{2+}a_3^{3+}$(ox Cu) + $a^{2+}a_3^{2+}$). Additional experiments will be required terpretations of the second-order dependence of the slow phase are also possible. One such interpretation is that the deviation of the slow phase from (pseudo-)first-order behavior is due to the presence of two first-order decays with similar (but not identical) rate constants. However, the excellent second-order fits place severe restrictions on the relative values of such rate constants; and, for this reason, the second-order interpretation is preferred.
(33) Wherland, S.; Gray, H. B. "Biological Aspects of Inorganic Chemistry", Addison, A. W., Cullen, W., James, B. R., Dolphin, D., Eds.; Wiley: New York, 1977; p 289.
(34) Holwerda, R. A.; Wherland, S.; Gray, H. B. *Annu. Rev. Biophys. Bioeng.* **1976**, *5*, 363.

Models for the Active Site of Oxygen-Binding Hemoproteins. Dioxygen Binding Properties and the Structures of (2-Methylimidazole)-*meso*-tetra($\alpha,\alpha,\alpha,\alpha$-*o*-pivalamidophenyl)porphyrinatoiron(II)–Ethanol and Its Dioxygen Adduct

Geoffrey B. Jameson,[1a] Frank S. Molinaro,[1a] James A. Ibers,*[1a] James P. Collman,*[1b] John I. Brauman,[1b] Eric Rose,[1b] and Kenneth S. Suslick[1b,c]

Contribution from the Departments of Chemistry, Northwestern University, Evanston, Illinois 60201, Stanford University, Stanford, California 94305, and University of Illinois, Urbana, Illinois 61801. *Received August 1, 1979*

Abstract: When crystals of (2-methylimidazole)-*meso*-tetra($\alpha,\alpha,\alpha,\alpha$-*o*-pivalamidophenyl)porphyrinatoiron(II)-ethanol, Fe(TpivPP)(2-MeIm)·EtOH, are exposed to dioxygen, the crystals of the resultant dioxygen adduct are still suitable for diffraction studies. The direct, precise determination of the stereochemical changes accompanying oxygenation of an iron(II)-(porphyrinato)(base) complex has been carried out using conventional X-ray diffraction methods. The structures have been refined by full-matrix, least-squares methods, using 4176 and 5183 reflections for the deoxy and oxy complexes, respectively, to R indices on F^2 of 0.162 and 0.120. For the portion of data where $F_o^2 > 3\sigma(F_o^2)$ the respective indices on F are 0.086 and 0.083. Crystal data for the deoxy compound follow: space group C_{2h}^6-$C2/c$, $Z = 4$, molecular symmetry C_2, $a = 18.871$ (11) Å, $b = 19.425$ (13) Å, $c = 18.434$ (11) Å, $\beta = 91.48$ (3)°, $V = 6755.0$ Å^3. The oxy complex is nearly isomorphic with $Z = 4$ in space group $C2/c$ with a cell of dimensions $a = 18.864$ (5) Å, $b = 19.451$ (5) Å, $c = 18.287$ (5) Å, $\beta = 91.45$ (2)°, $V = 6707.0$ Å^3. Some selected parameters for the coordination spheres, with those in square brackets pertaining to the dioxygen adduct, follow: Fe–N_{porph} = 2.068 (5), 2.075 (5) [1.997 (4), 1.995 (4)] Å; Fe–N_{Im} = 2.095 (6) [2.107 (4)] Å. The iron atom is displaced 0.399 [0.086] Å from the least-squares plane of the porphinato nitrogen atoms toward the imidazole ligand. The Fe–O separation is 1.898 (7) Å. The average O–O separation is 1.22 (2) Å and the Fe–O–O angle is 129 (1)°. In the presence of ethanol the deoxy complex binds dioxygen reversibly, noncooperatively, and with lower affinity than when the sample is desolvated—in the latter case dioxygen uptake has been found to be cooperative. The structure and properties of these possible models for T-state deoxy- and oxyhemoglobin are correlated and then compared with the 1-methylimidazole analogue. The sterically active 2-methyl substituent appears to perturb the Fe–O bond but not the Fe–N_{Im} bond.

Introduction

The structural changes which occur at the heme center upon the binding of dioxygen, carbon monoxide, nitric oxide, and alkyl isocyanides to hemoglobins, normal and abnormal, are of great importance to an understanding of structure-function relationships. In particular, discussions on the mechanism of cooperativity in the binding of small molecules to hemoglobin have been strongly influenced by structural data and physical measurements obtained from simple model systems;[2-8] this influence is manifested in the evolving concepts of Perutz.[9,10] In the absence of precise data from protein crystal structures, an absence that arises not from faults in the experiment but is intrinsic in the nature of the problem, model complexes have been invaluable as a means of establishing the general geometry of small molecule–hemoglobin complexes[11-15] and of understanding some general structure-function relationships.

Complexes of Fe(TPP)(1-MeIm)[16] with small molecules (O_2, CO, and NO) can be taken as models for the corresponding myoglobin adducts or for hemoglobin in the R (or high ligand affinity) states as the binding properties of the base, 1-methylimidazole, closely resemble those of the biological axial base, histidine. The recent studies of abnormal hemoglobins, with either unusually high or low ligand affinities,[17] are of considerable use in understanding the behavior of normal hemoglobins. It is often difficult to find appropriate model analogues. But by adding a sterically active substituent to the axial base, such as exists in 2-methylimidazole,[4b,18,19] or by creating steric strain in a covalent chain linking an imidazole base to the porphyrin skeleton,[20] affinities for small molecules are reduced. These systems at least mimic if not model low-affinity hemoglobins or T-state hemoglobin.[5,18,20,21] A very close structural correspondence between such model compounds and the metal sites of oxygen-binding hemoproteins has been established using techniques such as Mössbauer,[22-24] extended X-ray absorption fine structure (EXAFS),[6] resonance Raman spectroscopy,[25,26] and infrared spectroscopy.[27,28]

0002-7863/80/1502-3224$01.00/0